

Validation of the Energy Method to Predict the Liquefaction Potential of Soil Deposits through Case History Analysis

Mingjiang Tao,
Post Doctoral Researcher, Louisiana State University,
Baton Rouge, LA

J. Ludwig Figueroa and. Adel S. Saada
Dept. Of Civil Engineering,
Case Western Reserve
University, Cleveland, OH

OUTLINE

- **INTRODUCTION**
- **NUMERICAL INTEGRATION PROCEDURE**
- **CASE HISTORY VERIFICATION**
 - **Non Liquefaction Case**
 - **Liquefaction Case**
- **SUMMARY AND CONCLUSIONS**

INTRODUCTION

Previous Research:

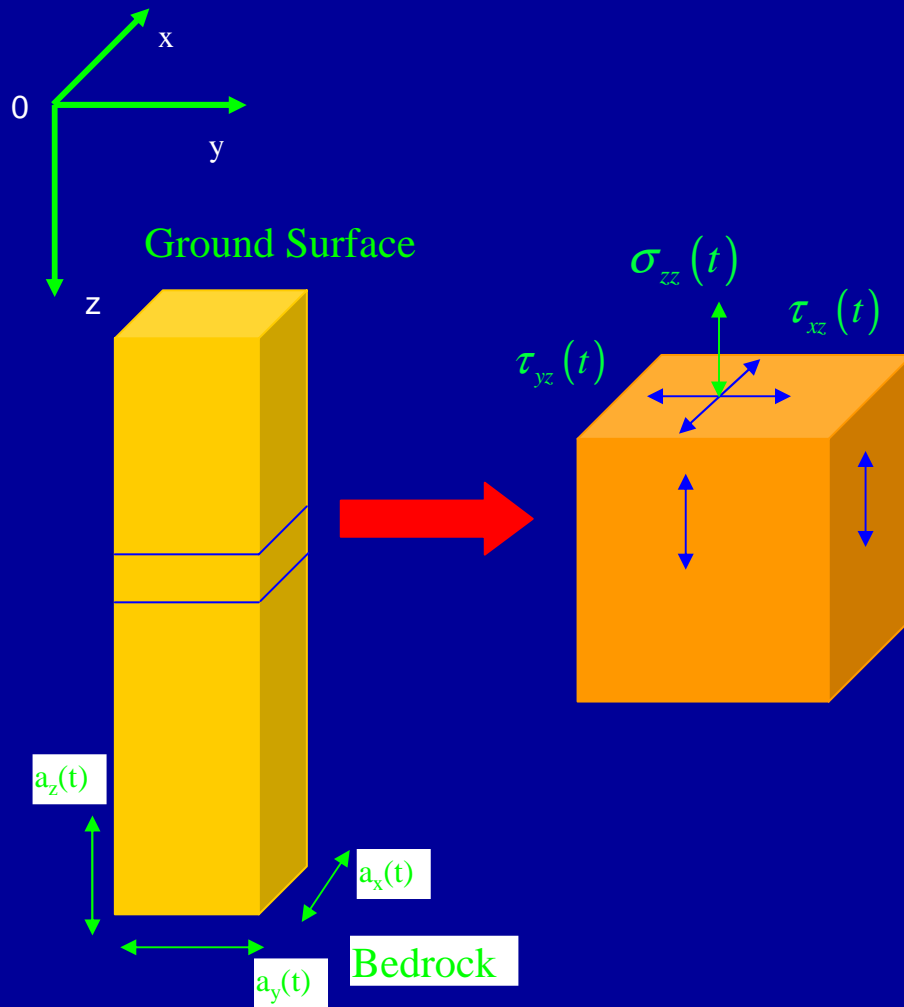
1. Liquefaction Resistance of sands was defined in terms of the Unit Energy using Torsional Shear Testing
 - a. Found that the Unit Energy was independent of type of loading whether harmonic or random
 - b. Developed relationships between the Unit Energy (dep. variable) and Effect. Conf. Pressure, Relative Density and Grain Size Characteristics
2. Developed a Unit energy-based one-dimensional analytical model to reconstruct in-situ soil behavior from which the induced level of energy could be determined.
 - Liquefaction susceptibility could be determined by comparing the induced vs. the resistant level of energy
3. Developed relationships to reconstruct the pore pressure buildup using the Unit Energy.

Previous Research (cont):

4. Developed relationships to calculate degradation parameters based on the Unit Energy. They allow the reconstruction of the time history of shear strength and shear modulus
5. Conducted a validation study of the energy method using dynamic centrifuge tests.
6. Tested hollow cylinder sand with significant amount of silt specimens under torsional shear to determine their resistance to liquefaction in terms of the Unit Energy.
7. Conducted a field verification study using Case Histories

A modified numerical procedure
to estimate the seismic response
of level ground

A Modified Numerical Procedure



Stress-State of a Soil Element Subjected to Earthquake Loading

Equations of Motion

$$\left\{ \begin{array}{l} \rho(z) \frac{\partial^2 U(z,t)}{\partial t^2} - \frac{\partial \tau_{xz}(z,t)}{\partial z} = 0 \\ \rho(z) \frac{\partial^2 V(z,t)}{\partial t^2} - \frac{\partial \tau_{yz}(z,t)}{\partial z} = 0 \\ \rho(z) \frac{\partial^2 W(z,t)}{\partial t^2} - \frac{\partial \sigma_{zz}(z,t)}{\partial z} = 0 \end{array} \right. \quad (20)$$

Boundary conditions:

$$\left\{ \begin{array}{l} \tau_{xz}(0,t) = 0 \\ \tau_{yz}(0,t) = 0 \end{array} \right. \quad \begin{array}{l} \text{At the ground} \\ \text{surface} \end{array} \quad (21)$$

$$\left\{ \begin{array}{l} U(0,t) = U_x(t) \\ V(0,t) = U_y(t) \end{array} \right. \quad \begin{array}{l} \text{At the bedrock} \end{array} \quad (22)$$

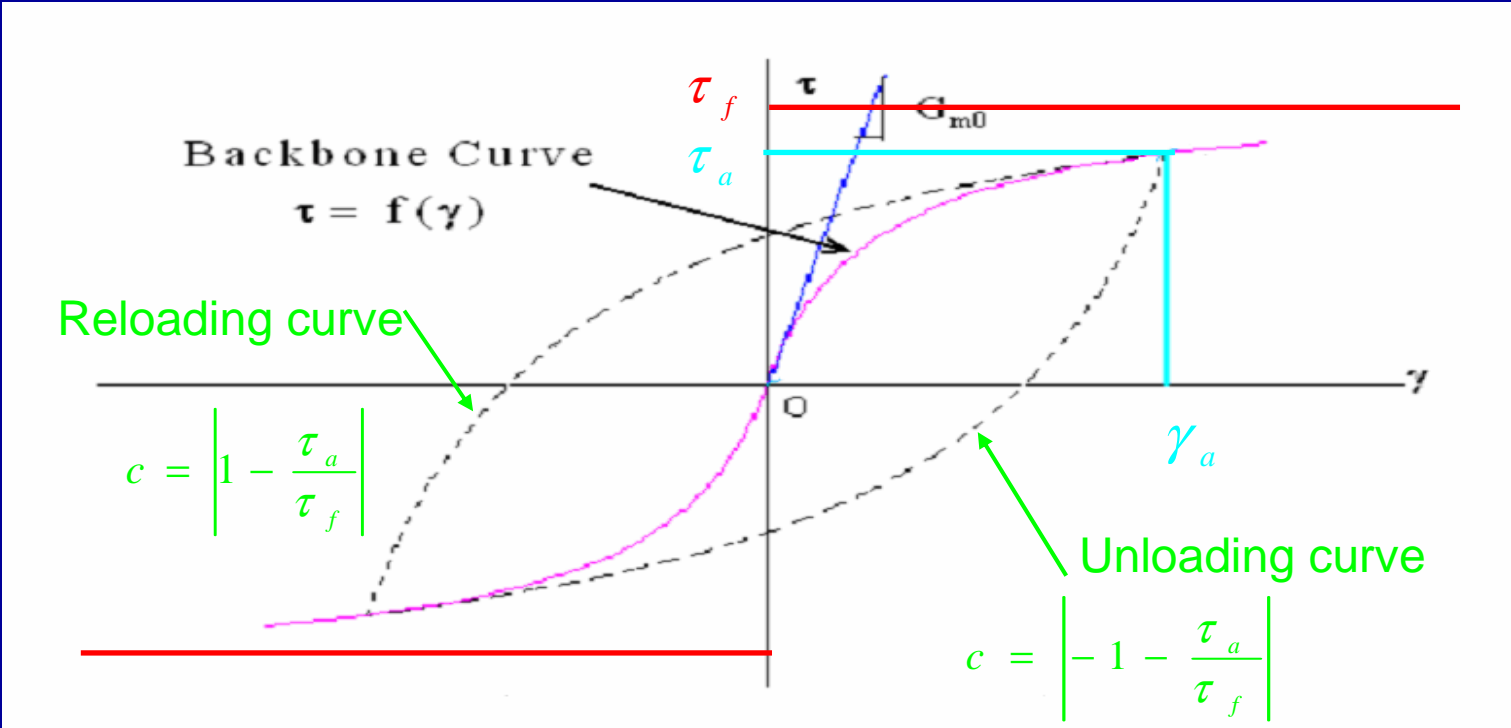
Hysteretic loops: generally consisting of the backbone, the unloading and reloading branches

Backbone curve: Hyperbolic model

$$\tau = \frac{G_m \gamma}{1 + \frac{G_m}{\tau_f} \gamma} = f(\gamma) \quad (23)$$

Unloading and reloading curves:

$$\frac{\tau - \tau_a}{c} = \frac{G_m \frac{\gamma - \gamma_a}{c}}{1 + \frac{G_m}{\tau_f} \left| \frac{\gamma - \gamma_a}{c} \right|} \quad (24)$$



Modified degradation models for shear modulus and shear strength:

$$\left\{ \begin{array}{l} G_{mt} = G_{m0} \left(1 - A_1 \frac{\delta W}{\sigma'_c} \right) \\ \tau_{ft} = \tau_{f0} \left(1 - A_1 \frac{\delta W}{\sigma'_c} \right) \end{array} \right. \quad \begin{array}{l} G_{mt}/G_{m0} \geq 0.9 \\ \tau_{ft}/\tau_{f0} \geq 0.9 \end{array} \quad (25)$$

$$\left\{ \begin{array}{l} G_{mt} = G_{m0} \left(1 - A_2 \frac{\delta W}{\sigma'_c} - B_2 \right) \\ \tau_{ft} = \tau_{f0} \left(1 - A_2 \frac{\delta W}{\sigma'_c} - B_2 \right) \end{array} \right. \quad \begin{array}{l} G_{mt}/G_{m0} < 0.9 \\ \tau_{ft}/\tau_{f0} < 0.9 \end{array} \quad (26)$$

A numerical solution based on Finite Difference Method (Take X direction as an example)

$$\begin{aligned}
 m_j \ddot{U}_{j,t+\Delta t} &= \tau_{j,t} - \tau_{j+1,t} = f(\gamma_{j,t}) - f(\gamma_{j+1,t}) \\
 &= F(U_{j-1,t}, U_{j,t}, U_{j+1,t})
 \end{aligned}
 \tag{27}$$

Calculate one time step from t_n to t_{n+1}

$$\left.
 \begin{aligned}
 k_1 &= \Delta t F(U^n, \dot{U}^n, t_n) \\
 k_2 &= \Delta t F\left(U^n + \frac{1}{2}\Delta t \dot{U}^n, \dot{U}^n + \frac{1}{2}k_1, t_n + \frac{1}{2}\Delta t\right) \\
 k_3 &= \Delta t F\left(U^n + \frac{1}{2}\Delta t\left(\dot{U}^n + \frac{1}{2}k_1\right), \dot{U}^n + \frac{1}{2}k_2, t_n + \frac{1}{2}\Delta t\right) \\
 k_4 &= \Delta t F\left(U^n + \Delta t\left(\dot{U}^n + \frac{1}{2}k_2\right), \dot{U}^n + k_3, t_n + \Delta t\right) \\
 U^{n+1} &= U^n + \Delta t\left[\dot{U}^n + (k_1 + k_2 + k_3)/6\right] \\
 \dot{U}^{n+1} &= \dot{U}^n + [k_1 + 2(k_2 + k_3) + k_4]/6 \\
 \ddot{U}^{n+1} &= F(U^{n+1}, \dot{U}^{n+1}, t_{n+1})
 \end{aligned}
 \right\}
 \tag{28}$$

Procedure summary:

- Input: soil properties, degradation parameters, Initial conditions:

$$G_{mj}^0 \quad \rho_j \quad \tau_{ff}^0 \quad U_j^0 = 0 \quad \tau'_{N+1} = 0$$

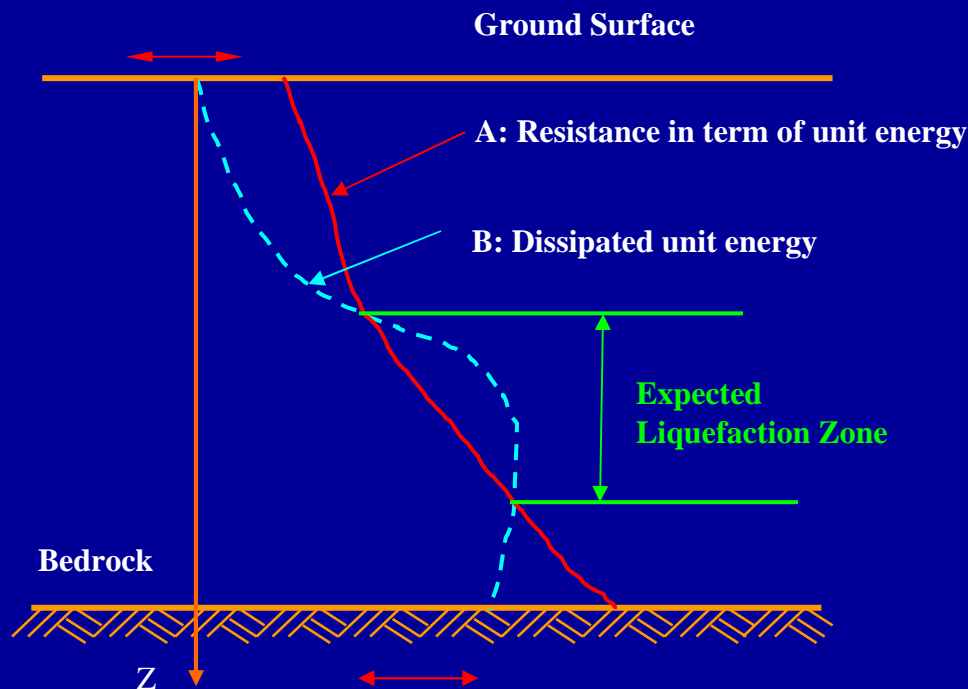
- At the beginning of each time step, V_j^t U_j^t are known at each layer boundary;
- The shear strain in the jth layer at time, γ_j^t can be obtained by using $\gamma_{j,t} = \frac{U_{j,t} - U_{j-1,t}}{h_j}$
- The unloading and reloading curves can be constructed by using Eq. (24);
- Calculate the dissipated unit energy due to the EW and the NS components individually, and then add them up;
- Update the shear modulus and strength at each reversal loading point;
- Repeat the above steps until the duration of the earthquake is over.

A Step-by-Step Energy-Based Procedure to Assess Liquefaction Potential of Soil Deposits

Step 1) Determination of the liquefaction resistance in terms of the unit energy

Step 2) Determination of the Amount of Dissipated Unit Energy into the Soil during the Expected Earthquake

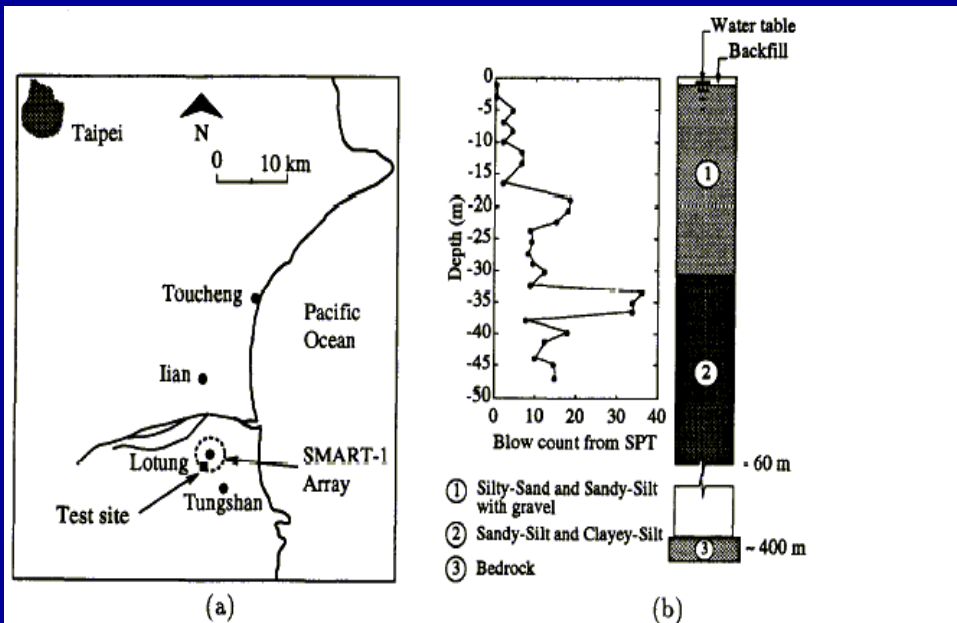
Step 3) Determination of the Liquefaction Potential



Case History Verification

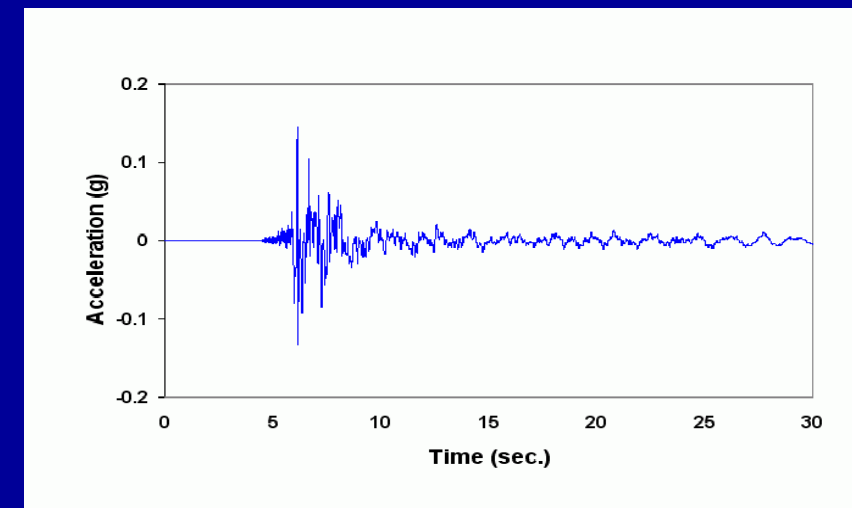
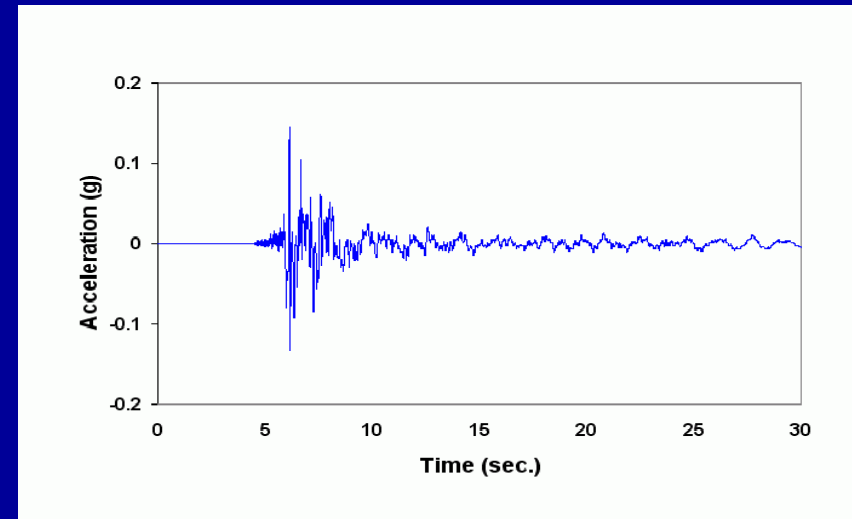
Non Liquefaction Case

(Lotung site, the 1986 LSST 12)



LSST Site: (a) Site Location; (b) SPT Log and Soil Profile (After Moh et al., 1988)

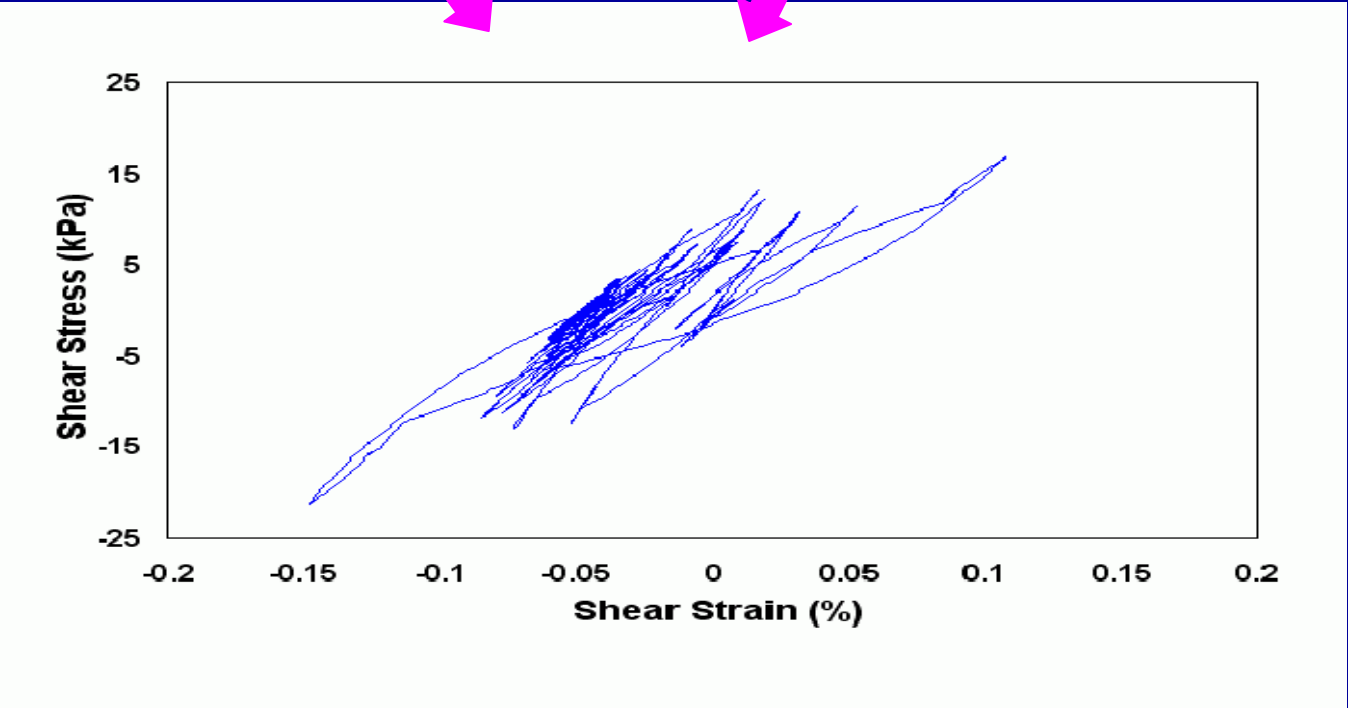
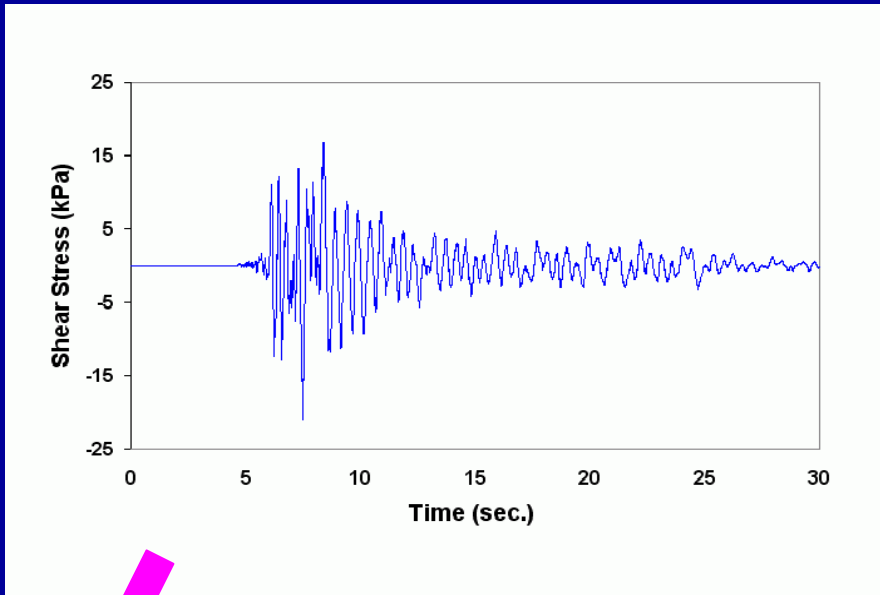
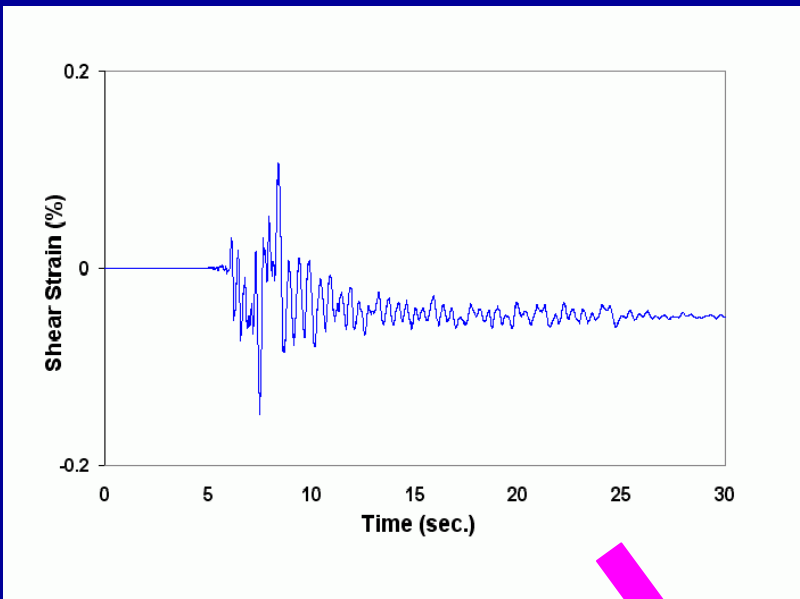
Input Excitation

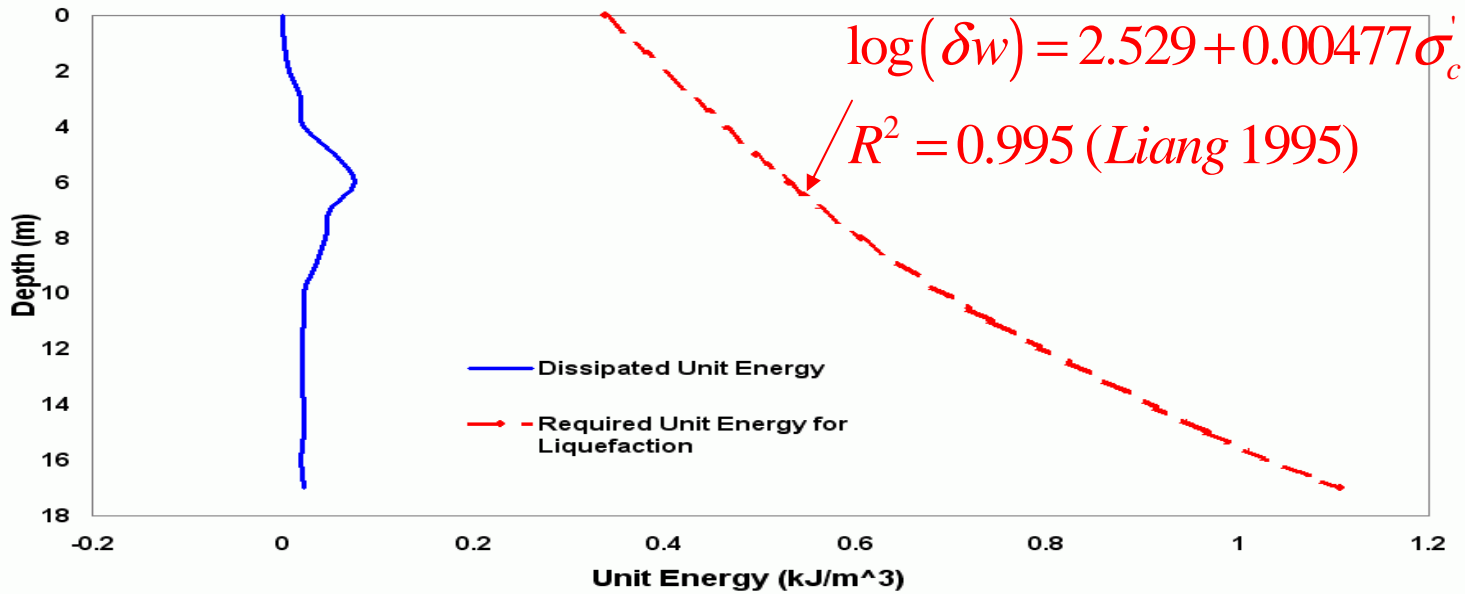
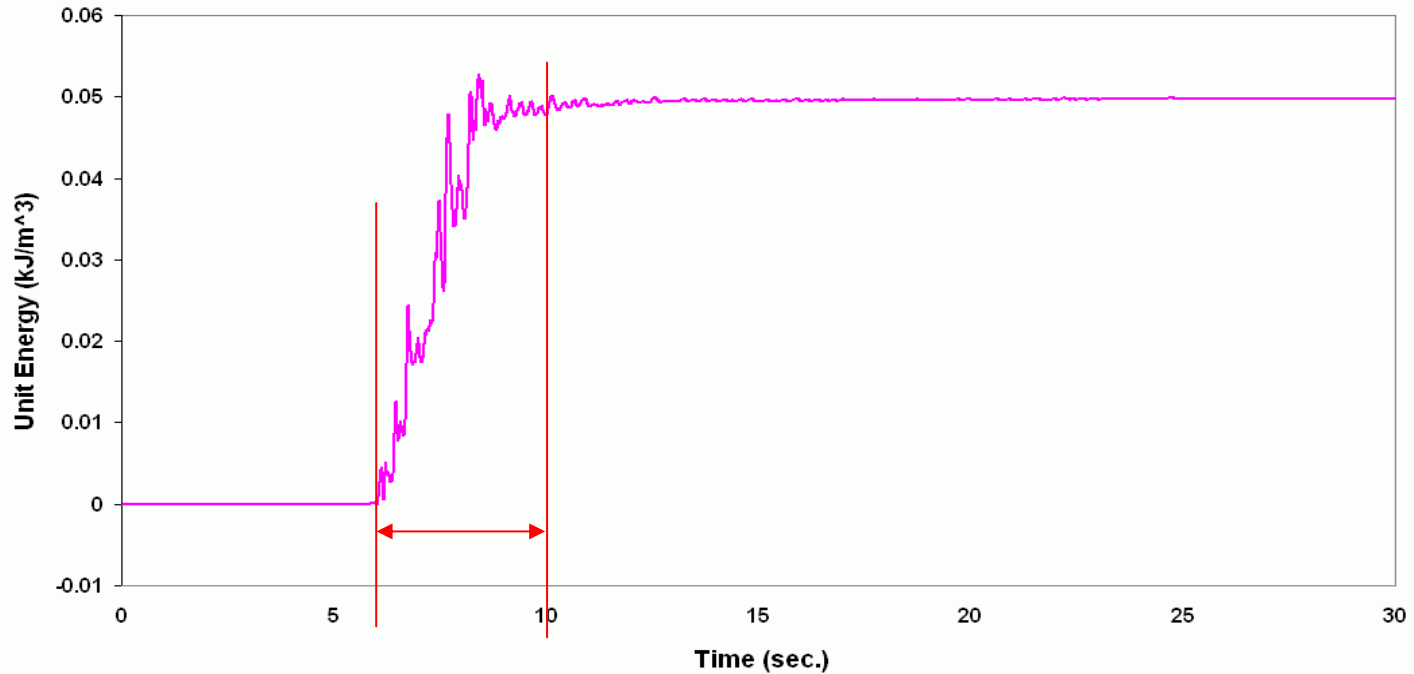


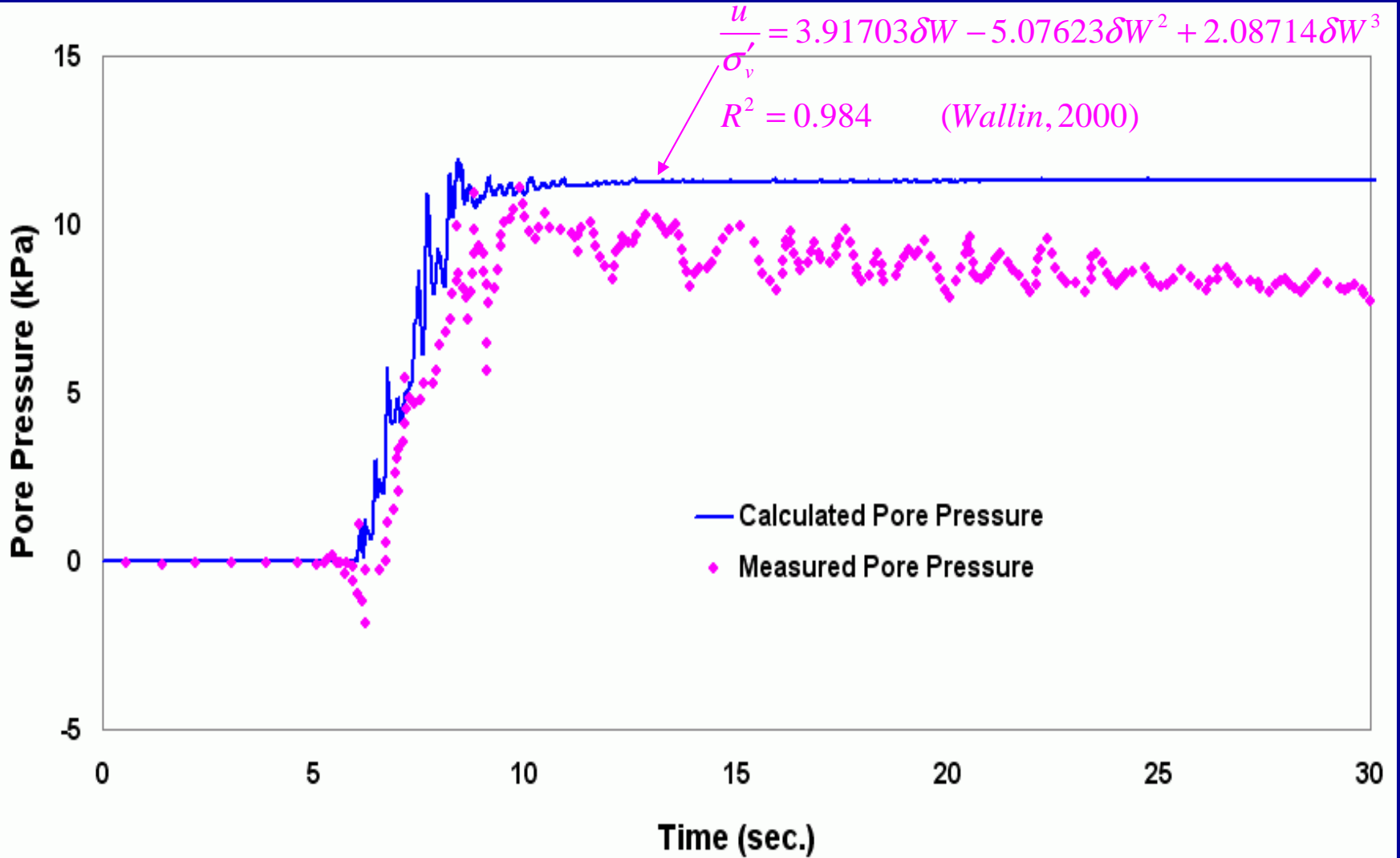
Recorded Acceleration Time Histories at 17 m Depth during LSST12 Event: (a) EW Component; (b) NS Component

Dynamic Properties and Degradation Parameters Used in the Analysis (Nonliquefaction Case)

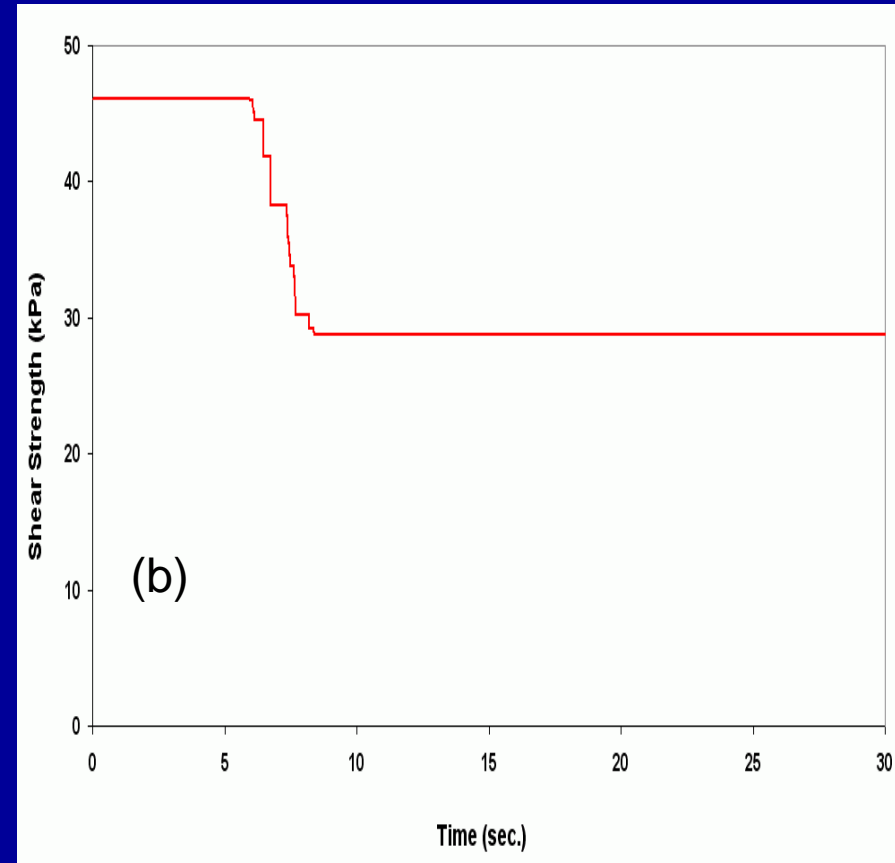
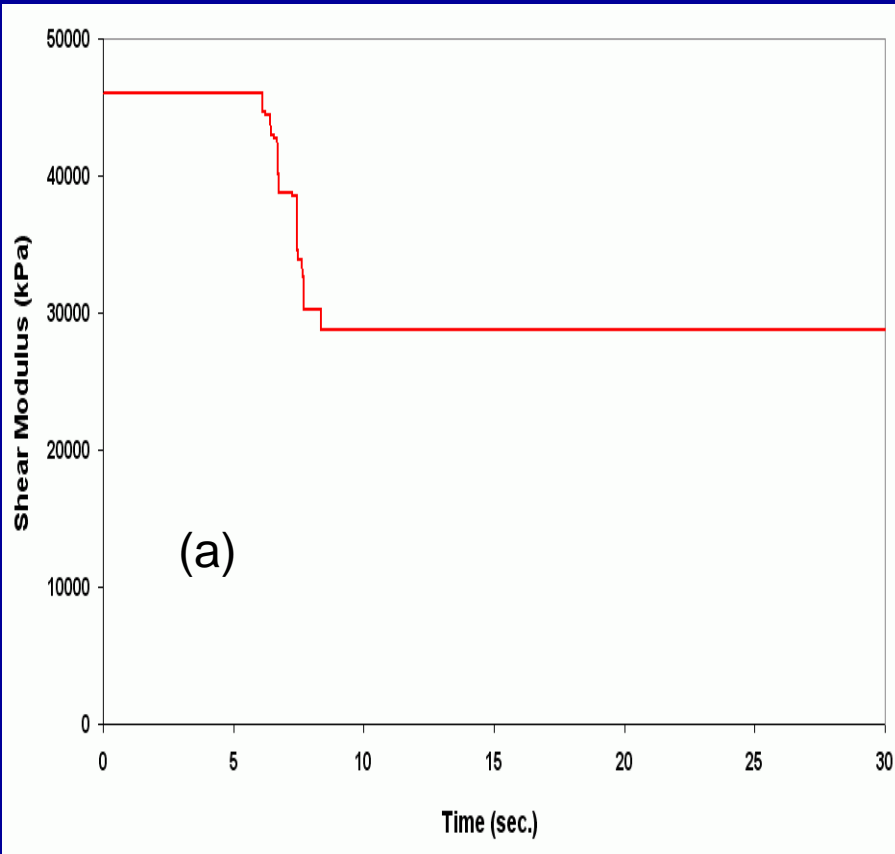
Layer No.	Thickness H (m)	Unit weight (kN/m ³)	G_{m0} (kPa)	τ_{f0} (kPa)	A ₁	A ₂	B ₂	ϕ
1	1.0	19.0	96709.830	96.71	320.0	10.0	0.84	30.0
2	1.0	19.0	88815.150	88.82	320.0	10.0	0.84	30.0
3	1.0	19.0	80262.580	80.26	320.0	10.0	0.84	30.0
4	1.0	19.0	75657.350	75.66	320.0	10.0	0.84	30.0
5	1.0	19.0	71052.120	71.05	320.0	10.0	0.84	30.0
6	1.0	19.0	67104.780	67.10	320.0	10.0	0.84	30.0
7	1.0	19.0	61841.660	61.84	320.0	10.0	0.84	30.0
8	1.0	19.0	57894.320	57.89	320.0	10.0	0.84	30.0
9	1.0	19.0	53289.090	53.29	320.0	10.0	0.84	30.0
10	1.0	19.0	47368.080	47.37	320.0	10.0	0.84	30.0
11	1.0	19.0	46052.300	46.05	320.0	10.0	0.84	30.0
12	1.0	19.0	42104.960	42.10	350.0	10.0	0.84	30.0
13	1.0	19.0	38157.620	38.16	350.0	10.0	0.84	30.0
14	1.0	19.0	34210.280	34.21	350.0	10.0	0.84	30.0
15	1.0	19.0	29605.050	29.61	350.0	10.0	0.84	30.0
16	1.0	19.0	24999.820	24.50	350.0	10.0	0.84	30.0
17	1.0	16.0	23026.150	23.03	350.0	10.0	0.84	30.0





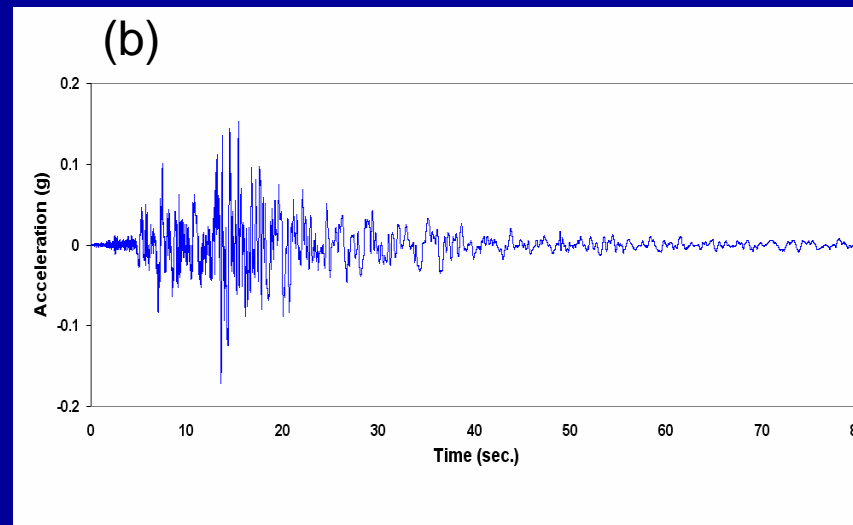
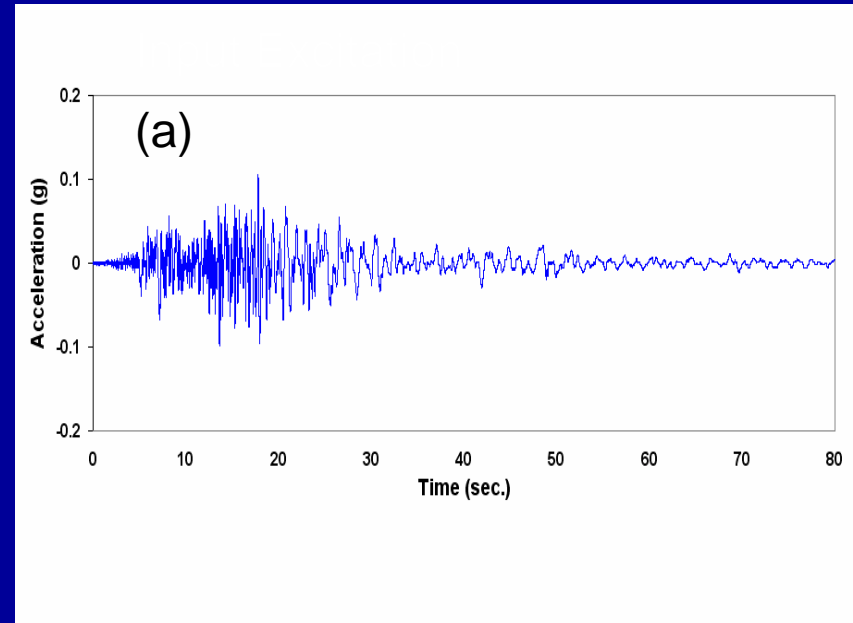
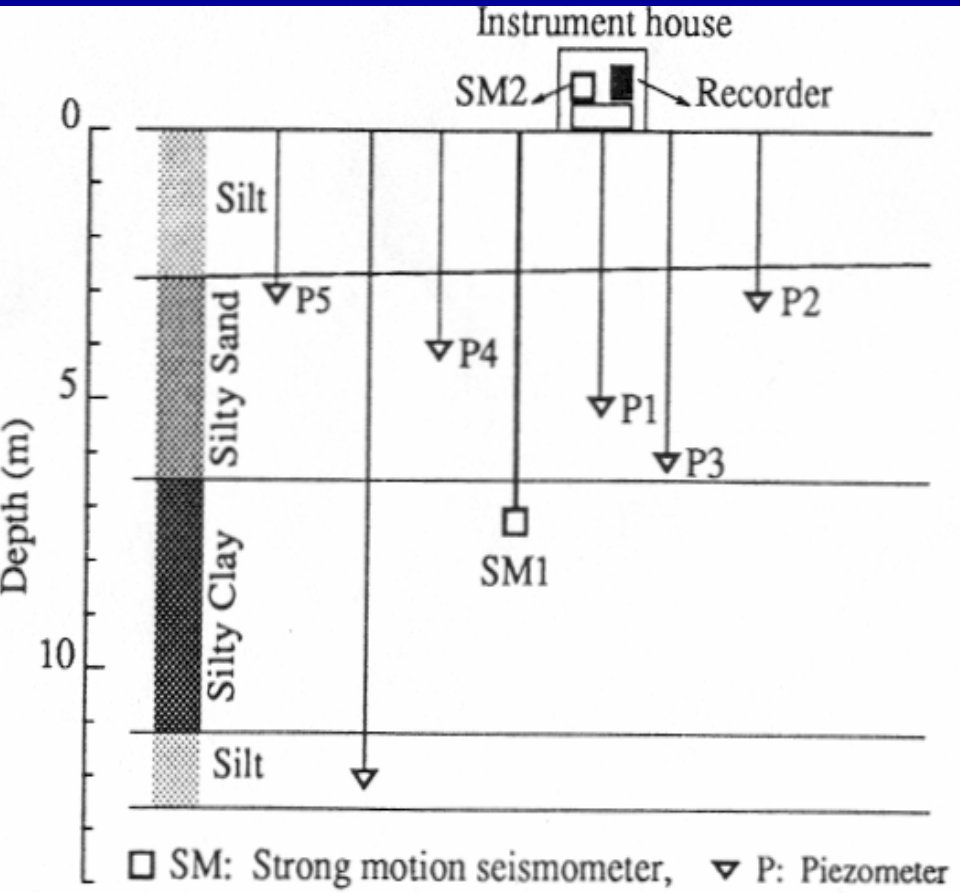


Comparison of the Calculated and Measured Pore Water Pressure at a Depth of 6.3 m (Lotung, 1986 LSST12 Event)



(a) Degradation of Shear Modulus at 6.3 m Depth; (b) Degradation of Shear Strength at 6.3 m Depth (during LSST12)

Liquefaction Case: Wildlife Site, the 1987 Superstition Hills Earthquake

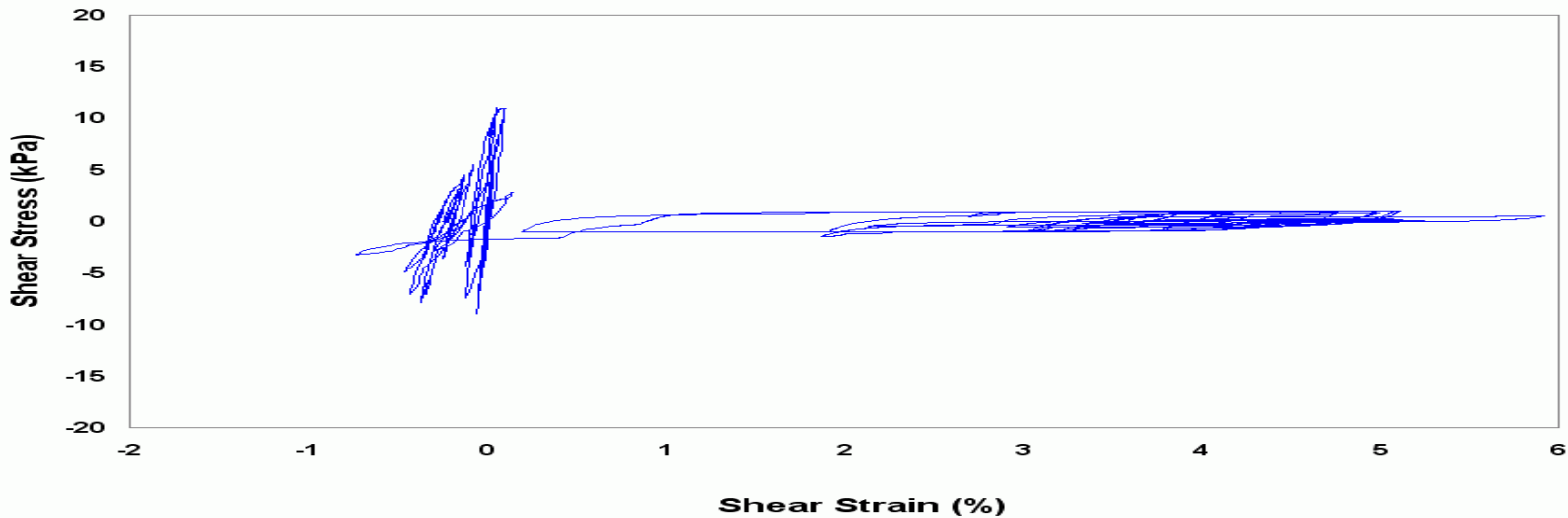
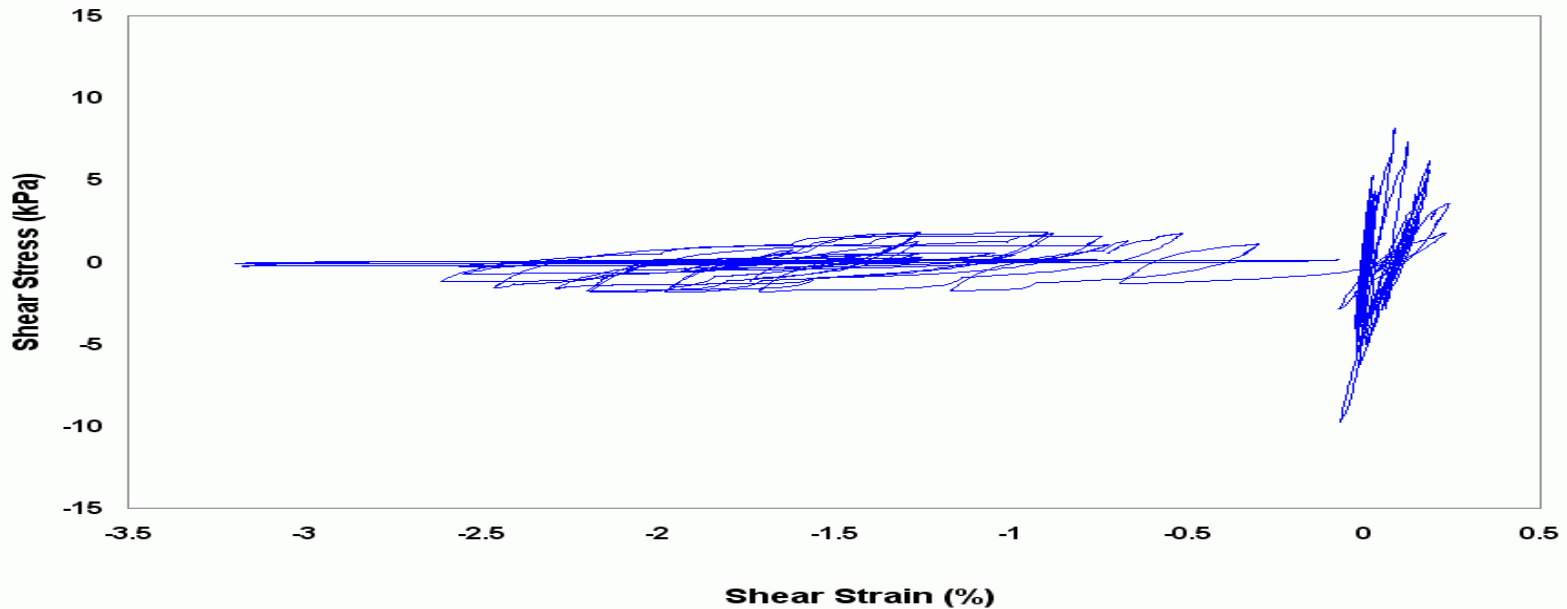


Cross Section and Instrumentation at the Wildlife Site (after Bennett et al. 1984)

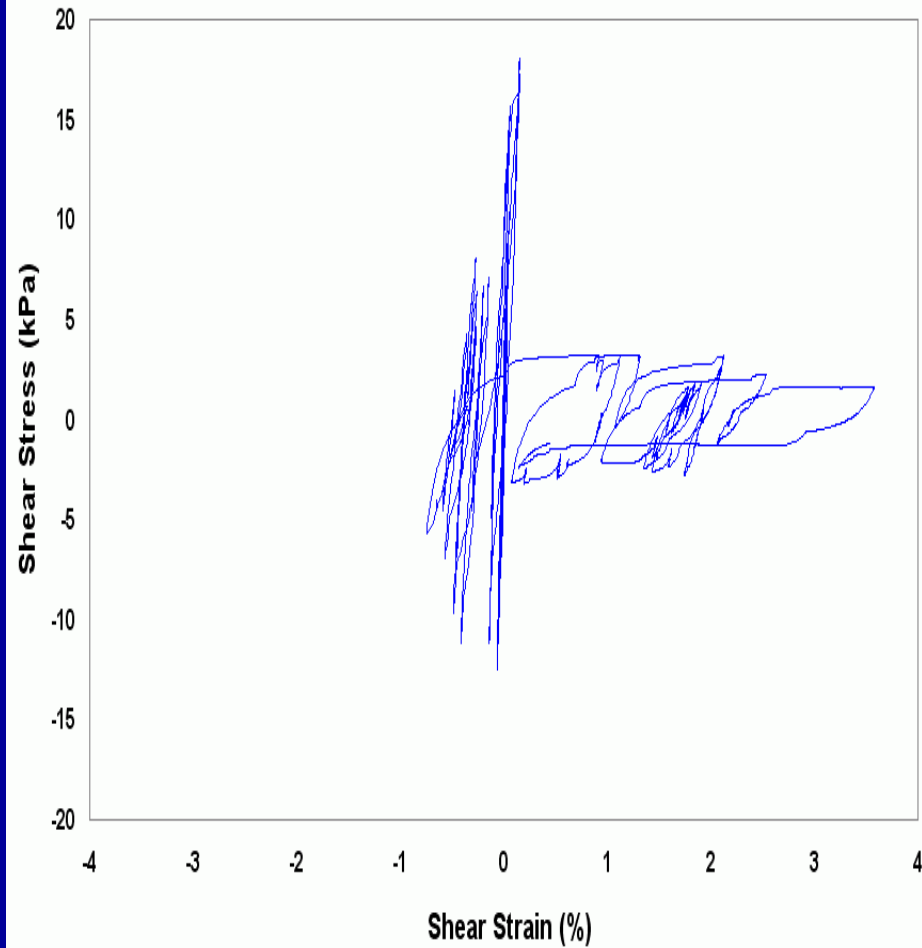
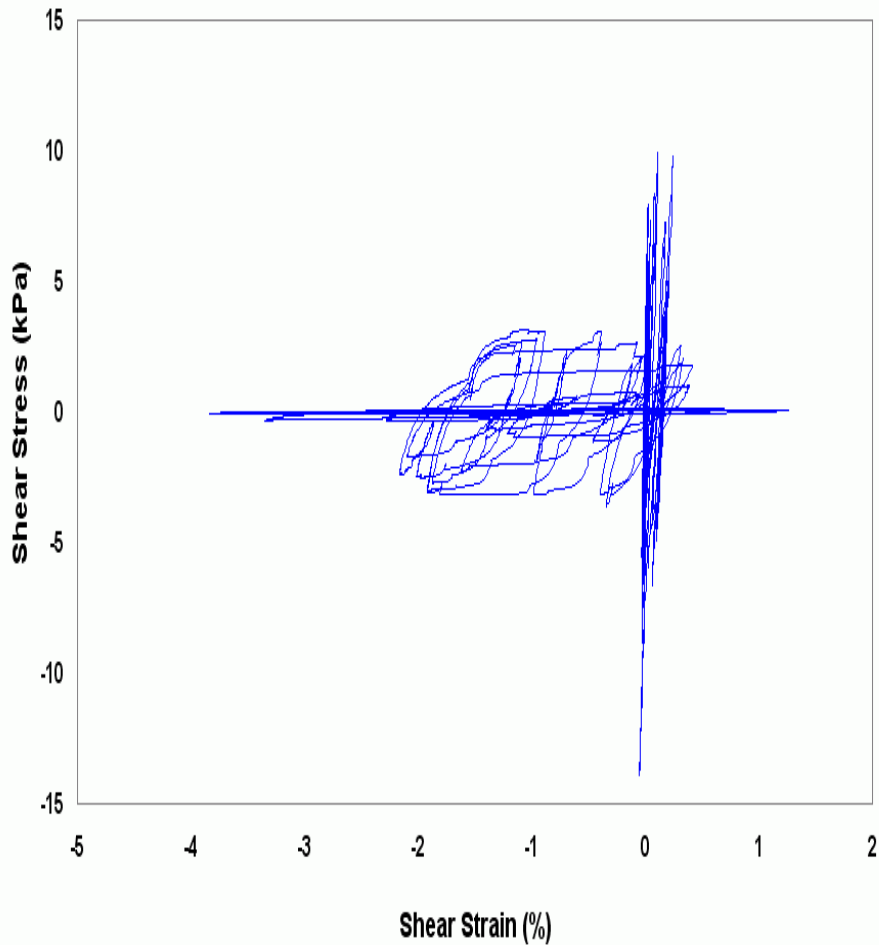
Recorded Acceleration Time Histories at a Depth of 7.5 m (1987 Superstition Hills Earthquake): (a) East-West (EW) Component; (b) North-South (NS) Component

Dynamic Properties and Degradation Parameters Used in the Analysis (Liquefaction Case)

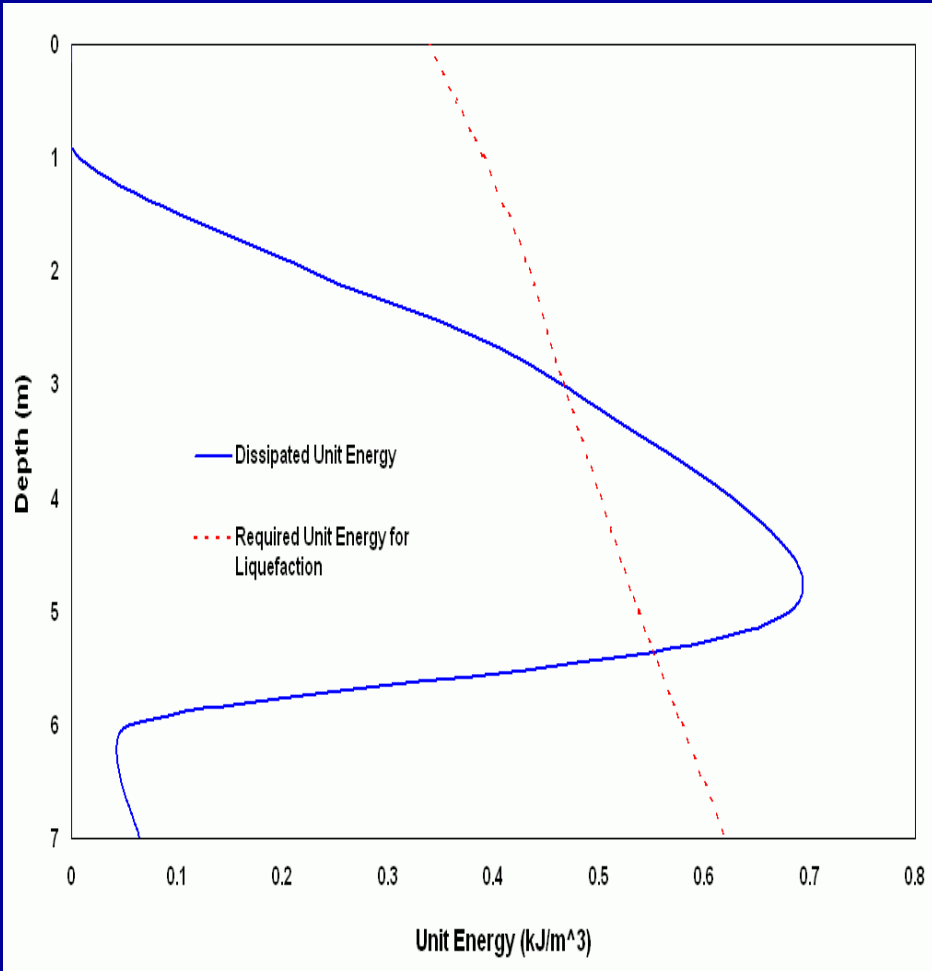
Layer No.	Thickness H (m)	Unit Weight (kN/m ³)	G_{m0} (kPa)	τ_{f0} (kPa)	A_1	A_2	B_2	ϕ
1	1.0	19.64	46491.480	46.49	380.0	10.0	0.84	30.0
2	1.0	19.64	39261.602	39.26	400.0	10.0	0.84	30.0
3	1.0	19.64	32749.920	32.75	440.0	10.0	0.84	30.0
4	1.0	19.64	30643.200	30.64	460.0	10.0	0.84	30.0
5	1.0	19.64	25711.560	25.71	480.0	10.0	0.84	30.0
6	1.0	19.64	19008.360	19.01	485.0	10.0	0.84	30.0
7	1.5	19.64	16710.120	16.71	400.0	10.0	0.84	30.0



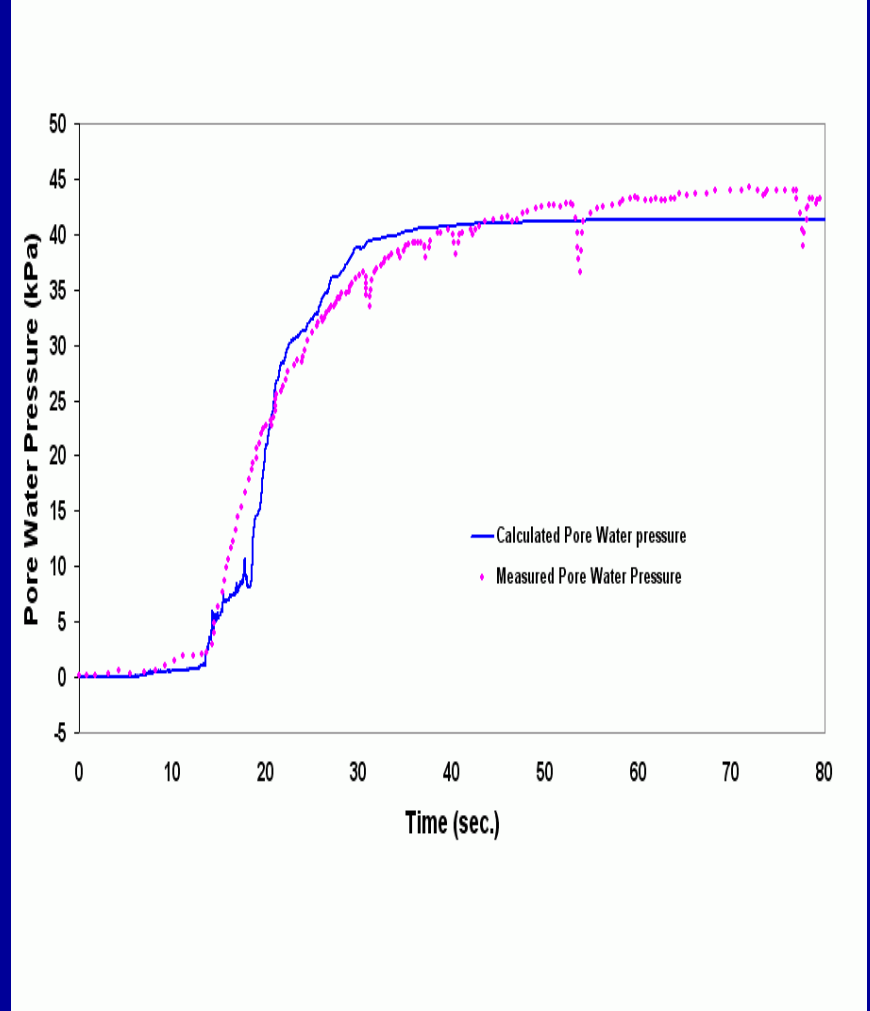
Calculated Shear Stress-Strain Curves at a Depth of 3.0 m (during the 1987 Superstition Hills Earthquake); (a) EW Component; (b) NS Component



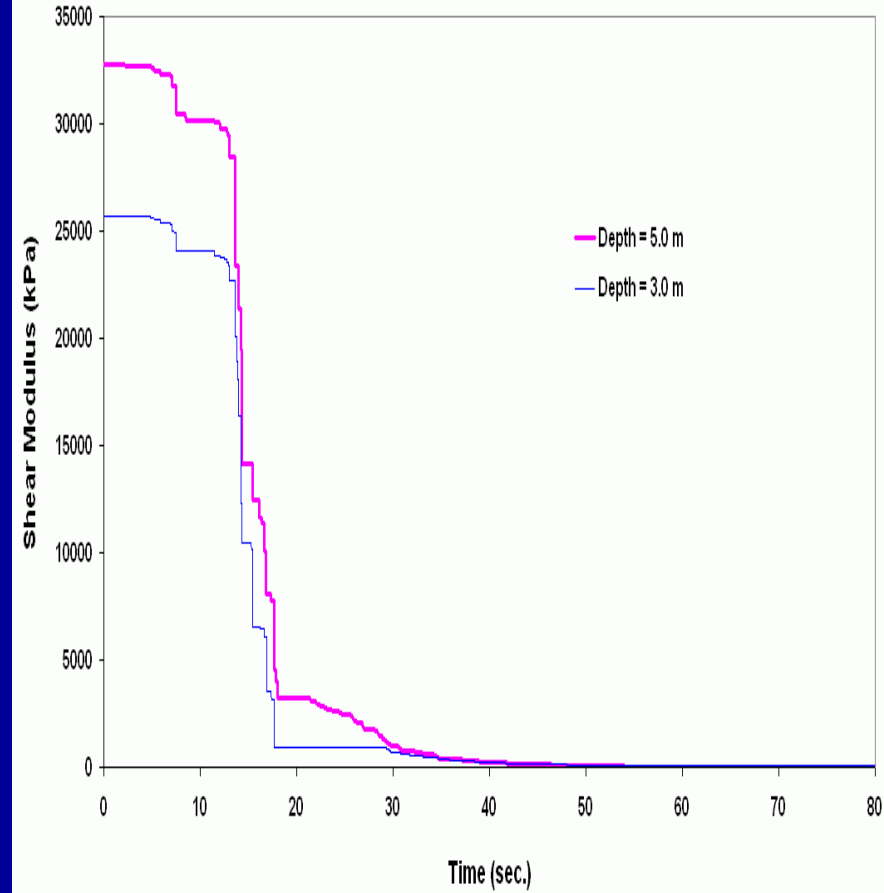
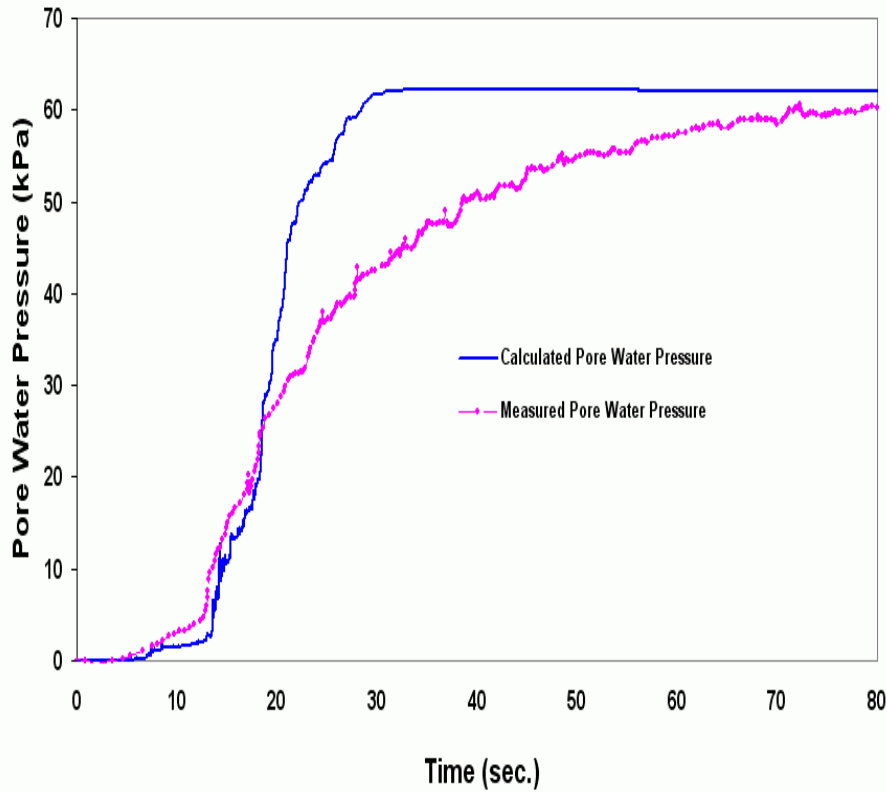
Calculated Shear Stress-Strain Curves at a Depth of 5.0 m (during 1987 Superstition Hills Earthquake); (a) EW Component; (b) NS Component



Comparison of the Calculated Dissipated Unit Energy and Required Unit Energy for Liquefaction (during the 1987 Superstition Hills Earthquake)



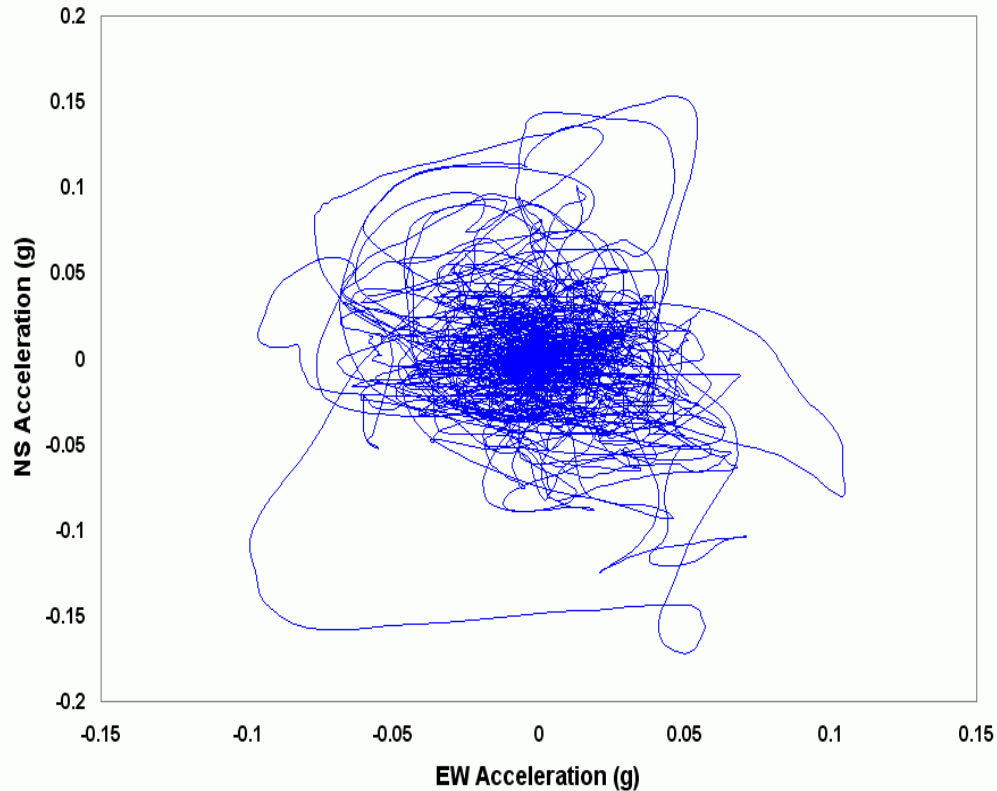
Comparison of the Calculated and Measured Pore Water Pressure at a Depth of 3.0 m (during the 1987 Superstition Hills Earthquake)



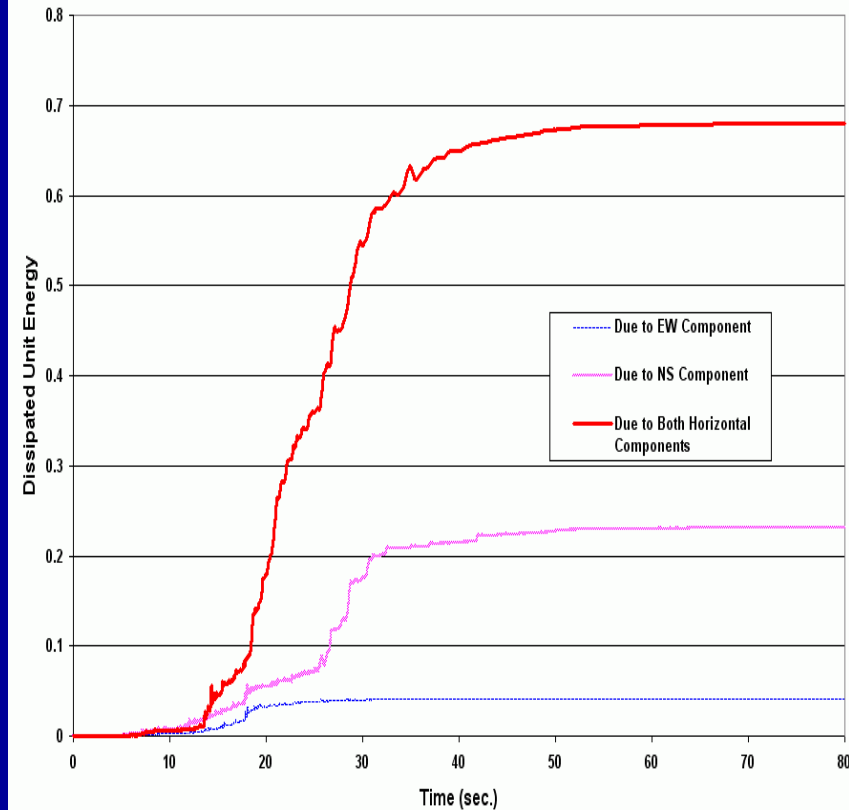
Comparison of the Calculated and Measured Pore Water Pressure at a Depth of 5.0 m (during the 1987 Superstition Hills Earthquake)

Degradation of Shear Modulus at Depths of 3.0 m and 5.0 m at Wildlife Site (during the 1987 Superstition Hills Earthquake)

Comparison of One-Dimensional and Two-Dimensional Analyses



Orbit of Recorded Acceleration at a Depth of 7.5 m from Wildlife Site (Superstition Hills Earthquake, 1987)



Comparison of Dissipated Unit Energy due to EW Component, NS Component, and Both Horizontal Components at a Depth of 5 m (Wildlife Site, 1987 Superstition Hills Earthquake)

Conclusions

■ Predictions obtained by the energy-based procedure were in very good agreement with actual field observations.

■ The validity of the energy-based pore pressure model was also supported by the agreement of the measured and calculated pore pressure time histories.

■ Comparison of one-dimensional and two-dimensional analyses suggested that both components of horizontal accelerations are significant and should be considered simultaneously while evaluating the liquefaction potential of soils.

■ It was shown that degradation parameters are dependent mainly on soil characteristics and site features.

QUESTIONS

